Research Article | Vol. 27, No. 19 | 16 Sep 2019 | OPTICS EXPRESS 26821
Optics EXPRESS

Pump absorption, laser amplification, and effective length in double-clad ytterbium-doped fibers with small area ratio

YUTONG FENG,[1,*] PABLO G. ROJAS HERNÁNDEZ,[1] SHENG ZHU,[1] JI WANG,[1] YUJUN FENG,[1] HUAIQIN LIN,[1] OSCAR NILSSON,[1,2] JIANG SUN,[1,3] AND JOHAN NILSSON[1]

[1]*Optoelectronics Research Centre, University of Southampton, Southampton, SO17 1BJ, UK*
[2]*Currently with the Department of Aeronautics, Imperial College London, London, SW7 2AZ, UK*
[3]*Currently with the China Academy of Electronics and Information Technology, Beijing, 100041, China*
[*]*y.feng@soton.ac.uk*

Abstract: We use numerical simulations with the beam propagation method (BPM) and rate equations to investigate the pump absorption and amplification characteristics in double-clad ytterbium-doped fibers with small cladding-to-core area ratios, in the range 1 -3. The presence of modes with low overlap with the doped region (or alternatively, skew rays) hampers the pump absorption in a circular geometry, but we find that the effect is small for area ratios of ~2.5 or less. We derive ray-based expressions for the small-signal absorption which show similar results. However, even when the small-signal absorption scales nearly ideally with the inverse of the area ratio, the absorption in an operating amplifier is much lower, and the dependence on the area ratio much weaker, when a large fraction of the Yb-ions is excited in a small-area-ratio fiber. We derive equations which show this, and that in contrast to conventional area ratios of, e.g., 100, the fiber length depends more strongly on the required gain than on the required pump absorption. However, fibers substantially shorter than 1 m still allow for adequate pump absorption and gain. The effective length for nonlinear interactions is less affected by this, since the Yb-excitation is low where the signal power is high. Although we treat single-mode cores, the BPM amplifier simulations show there are a few percent of the signal power in cladding-guided modes with high overlap with the Yb-doped core. Nevertheless, according to our simulations, it is possible to achieve high efficiency and mode purity with a small-area-ratio circularly symmetric double-clad fiber.

1. Introduction

Circular symmetry in double-clad fiber (DCF) doped with ytterbium or another rare earth is known to lead to poor overlap between helical pump modes in the inner cladding with the rare-earth-doped region in the core, and thus low effective pump absorption [1]. This is generally detrimental, e.g., because of increased nonlinear degradation and background loss if it leads to the use of a longer fiber, so several techniques such as noncircular inner cladding and offset signal core are used to perturb the circular symmetry and thus improve the pump absorption per unit length [2–4]. At the same time, the pump absorption in double-clad fiber is under some assumptions in some regimes approximately inversely proportional to the ratio of the inner cladding area to the area of the Yb-doped region, i.e., A_{clad}/A_{core} in case of a fiber doped throughout the core [5]. We consider this to be the ideal case. Decreasing this ratio is also a route to increased pump absorption and lower nonlinear degradation. Furthermore, a smaller area ratio can bring several additional benefits. For example, it can reduce the quantum defect in Yb-doped fiber lasers and amplifiers [6], enable efficient operation at 980 nm [7–9], and allows the Yb-concentration to be reduced, which may reduce photodarkening [10] and simplify control

#360079 https://doi.org/10.1364/OE.27.026821
Journal © 2019 Received 13 Feb 2019; revised 28 May 2019; accepted 28 May 2019; published 11 Sep 2019

Optics EXPRESS

of the refractive index in the fabrication process. However, all those benefits rely on the ability of a smaller area ratio to create a larger overlap between the pump and the dopant, and thus a higher absorption.

The area ratio between the cladding and the core can be decreased by increasing the core diameter. However this option is limited when single mode (SM) operation is required. It is also possible to reduce the inner-cladding size. Although this reduces the pump power that can be coupled into the cladding, the high brightness available today with diode lasers suitable for pumping as well as with alternative pumping schemes such as tandem-pumping [11] helps to overcome this limitation. However conventional double-clad fibers, in which a low-index polymer coating serves as the outer cladding, generally have inner-cladding diameters of ~125 µm or larger. In this type of fibers, this is then also the diameter of the glass structure. Thinner sizes are increasingly difficult to handle and susceptible to micro-bending [12]. Jacketed air-clad fibers [13, 14] offer an alternative route to small inner claddings, but involve silica:air micro-structuring which makes them more difficult to fabricate and handle, and impedes heatsinking.

All-glass waveguides, in which neither a silica:air microstructure nor the polymer coating plays a role in the waveguiding, is another option. Such fibers can have a low-refractive-index region (e.g., fluorine-doped) around an inner cladding of pure silica or an inner cladding with a raised refractive index surrounded by a pure-silica outer cladding [15]. However, it is more difficult to make the fiber non-circular, since conventional fabrication with modified chemical vapor deposition (MCVD) do not offer access to the inner cladding for machining, which may also be precluded by stress. It may still be possible to machine the outer cladding (typically made of pure silica) and rely on surface tension to distort the inner cladding during the fiber draw. However, geometries normally preferred for cladding-pumping (e.g., hexagons and other polygons) may be difficult to realize with this method. It also distorts the core, which may be undesirable. An unsuitable geometry (e.g., circular) may then compromise the scope for increasing the pump absorption through the use of a small inner cladding.

On the other hand, the fraction of the pump light with low overlap with the doped core vanishes for unity area ratio, i.e., when the inner cladding and core coincide, and it is intuitively clear that the fraction remains small for small area ratios. This reduces the need for a non-circular inner cladding for sufficiently small area ratios.

However, a small area ratio requires high-brightness pumping. Consequently, the potential brightness enhancement from pump to signal becomes smaller. The brightness enhancement also depends on the beam quality, or mode purity, of the generated light. A potential problem with a small inner cladding is that the mode purity may be degraded, if the number of modes with large overlap with the amplifying core, and which will therefore be present in the output beam, increases. In case of a small inner cladding, this may include cladding-modes.

In this paper, we use computer simulations to investigate the pump absorption, signal amplification, mode purity, and effective length for nonlinear interactions of circularly symmetric and non-circular double-clad fiber amplifiers with small area ratios and cores that are nominally single-mode. We use the beam propagation method (BPM) combined with standard rate equations to simulate co-directionally cladding-pumped high-power phospho-aluminosilicate ytterbium-doped fiber amplifier in the absence of mode-coupling. We find that a non-circular inner cladding does improve the pump absorption as it does with conventional double-clad fibers, but a circular inner cladding is nearly as good for area ratios up to approximately 2.5, corresponding to a diameter ratio of 1.6. We derive analytic expressions for the actual and effective length and compare them to the BPM simulations, and discuss the dependence on the core-to-cladding area ratio. In contrast to conventional double-clad fibers with larger area ratios, the reduction in fiber length is much smaller than the reduction in area ratio. We also discuss scaling of other fiber parameters. For computational reasons we use an artificially high Yb-concentration in short fibers, but have verified that the results can be scaled to longer fibers with lower Yb-concentration.

Optics EXPRESS

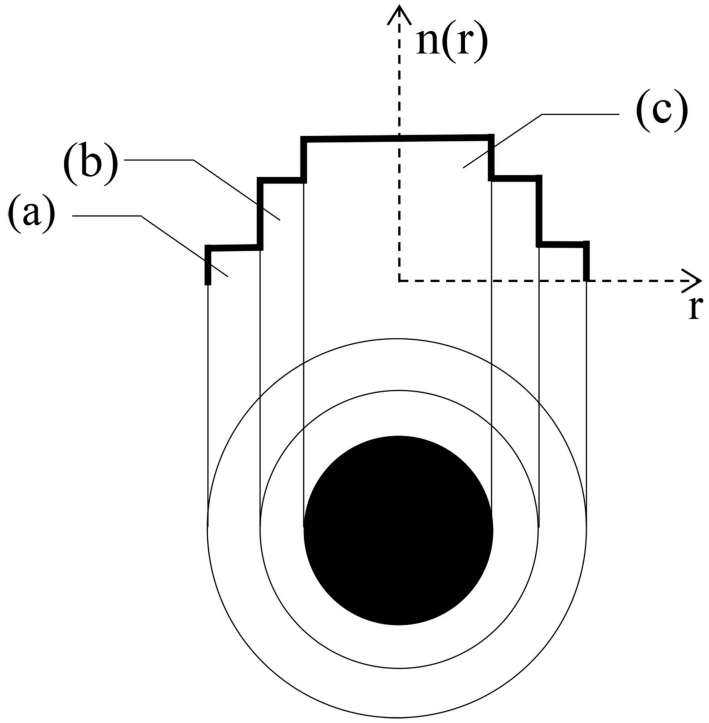

Fig. 1. Double-clad fiber structure under consideration. (a) outer cladding; (b) inner cladding; (c) core, which coincides with the Yb-doped region.

Therefore, although we report absolute fiber lengths, the relative lengths are arguably more significant. Whereas most of our results are for operating amplifiers in which a significant fraction of the Yb-ions is excited, we also use BPM to calculate the small-signal pump absorption (with no excited Yb-ions), and compare this to ray-based expressions, which we derive.

2. Numerical simulation method

Figure 1 shows the primarily considered double-clad fiber structure, with concentric step-index inner cladding and single-mode core, which is homogenously Yb-doped throughout. Table 1 lists the primarily considered parameters. We treat area ratios between the pump waveguiding region (inner cladding & core) and core in the range 1-3, where unity area ratio corresponds to core-pumping. We kept the index difference between core and outer cladding constant as the inner cladding vanishes, so at unity area ratio the structure transitions into a multimode step-index core with large numerical aperture (NA).

There are several approaches, e.g., modal treatments, to evaluate light propagation in such structures. We used the beam propagation method [16] (BPM) as implemented in RP Fiber Power for the scalar wave equation in the paraxial approximation to calculate the evolution of both the signal and the pump fields, at low as well as high powers. The pump and signal are assumed to propagate in the same direction. RP Fiber Power uses Fourier transformation to calculate the diffraction in the BPM. It also calculates the excitation of the Yb-ions by solving conventional rate equations, whereafter it calculates the local gain and absorption of the fields. The power in a specific mode and its evolution along the fiber are evaluated by calculating the overlap of the total signal field with the mode field of interest. RP Fiber Power also evaluates how the total signal and pump powers evolve along the fiber by integrating the respective intensities in

Optics EXPRESS

Table 1. Fiber and Simulation Parameters used in this paper unless otherwise stated

Parameter	Description	Value
λ_p	Pump wavelength	976 nm
λ_s	Signal wavelength	1060 nm
N_0	Yb concentration	6.5×10^{26} ion/m^3
D_{core}	Core diameter	15 µm
NA_{core}	Core NA	0.05
NA_{clad}	Clad NA	0.3
V	V-value of single-mode core	2.22
	Effective area of LP_{01} (with infinite inner cladding)	229 µm^2
	Area ratio between pumped region and core	1-3
	Inner-cladding diameter	21.2 µm (area ratio 2) 26.0 µm (area ratio 3)
	Approximate number of supported scalar pump modes (V^2/4)	53 (area ratio 1) 106 (area ratio 2) 158 (area ratio 3)
P_{signal}	Total launched signal power	100 mW
	Fraction of signal power launched into LP_{01}	95%
	Fraction of signal power launched into LP_{11}	5%
P_{pump}	Total launched pump power	30 W
σ_a	Absorption cross section	1.77×10^{-24} m^2 at 976 nm 8.02×10^{-27} m^2 at 1060 nm
σ_e	Emission cross section	1.71×10^{-24} m^2 at 976 nm 0.42×10^{-24} m^2 at 1060 nm
τ	Fluorescence lifetime	0.85 ms
	Pump absorption at zero excitation and unity overlap	5 dB/mm
	Small-signal ("cold") pump absorption length	0.87 mm (area ratio 1) 1.74 mm (area ratio 2) 2.61 mm
	Signal absorption at zero excitation and unity overlap	0.0227 dB/mm
	Signal intrinsic saturation intensity	0.515 mW/µm^2
	Signal intrinsic saturation power (based on core area)	91.0 mW

Optics EXPRESS

different transverse planes.

The results depend on the light excitation conditions. Unless otherwise stated, for amplification simulations, we use an input signal which consists of a mixture of the LP_{01}-mode and one of the two degenerate LP_{11}-modes and where 5% of the power is in LP_{11}. Note that this is a cladding-mode of the double-clad fibers. The phase difference between LP_{01} and LP_{11} is zero at launch, although this is not important since the phase difference varies rapidly along the fiber. The input pump is a mixture of all guided modes where each mode has the same power and a random phase for amplifier as well as small-signal absorption simulations. For the ray analysis of the small-signal absorption, we use an equivalent excitation with uniform power density at the fiber facet and with the direction of propagation uniformly distributed in the transverse plane in each point in the waveguiding region. But note that we use BPM unless otherwise stated.

Mode-coupling is neglected. Mode coupling increases the pump absorption by transferring power from modes with low absorption to those with high absorption. This suggests that the actual pump absorption may be higher. However, mode-coupling is expected to be small, and may be negligible, because of the relatively large modal effective-index spacings for the small inner claddings we consider.

Also amplified spontaneous emission (ASE) is neglected. Whereas ASE can be avoided at the low signal gain we consider, it can still be a factor if the gain peak wavelength is different than the signal wavelength, or the gain is locally unsaturated, e.g., at the edge of the core [10].

With our assumptions, there is no counter-propagating light. Therefore, the light-fields at any longitudinal fiber coordinate can be taken as the output light-field for a fiber of the corresponding length. This contrasts with the case when coupling between forward and backward-propagating light is significant, which is common at high levels of gain.

Because of the large computational burden of BPM, the simulated fiber lengths are short t. The Yb-concentration of 6.5×10^{26} ions/m^3 is artificially high to compensate for the short length, and may be unrealistic. A concentration of 1×10^{26} ions/m^3 is more typical for conventional double-clad Yb-doped fibers, and a lower-than-normal concentration of, say, 1×10^{25} ions/m^3 may be more appropriate for the area ratios we consider. A lower concentration helps to reduce thermal effects, which otherwise can be significant at high power. Note also that except for long-wavelength tandem-pumping, a small inner cladding typically leads to a high Yb-excitation, which can accelerate photodarkening [10] and may require an Yb-concentration that is lower than normal. However, our modeling excludes those effects, as well as nonlinearities such as stimulated Raman scattering. We verified that our results can be scaled to longer fibers of lower Yb-concentrations, in the absence of those effects. Thus, insofar as those effects are negligible, the simulated fibers are still long enough to accurately describes the pump absorption and laser amplification characteristics also in more typical lengths.

Note also that the use of BPM implies that pump and signal are both assumed coherent, whereas at least the pump is normally incoherent. However, we found only small differences between the coherent simulations presented here and incoherent simulations (also with RP Fiber Power and without mode-coupling).

3. Results and discussion

3.1. Small-signal pump absorption

Figure 2 shows the so-called small signal, or "cold", pump absorption, i.e., when all Yb-ions are in the absorbing ground state, for different inner-cladding shapes and for three different area ratios, where unity area ratio corresponds to core-pumping. In case of unity overlap, the absorption is given by the product of the concentration and absorption cross-section, and becomes 5.00 dB/mm. In case of cladding-pumping, because the distribution of the launched light is nearly uniform across the inner cladding, the initial rate of absorption is inversely proportional to the area ratio. The length-coordinate in Fig. 2 is scaled to compensate for this dependence and

Optics EXPRESS

thus facilitate comparisons of the deviations from the ideal exponential power decay according to Beer-Lambert's law. The rate of absorption decreases along the length of the double-clad fibers, since modes with high overlap with the Yb-doped core are preferentially absorbed in the initial part of the fiber, and relatively more of the remaining pump power is propagating in modes with small overlap with the Yb-ions. Also the core-pumped fiber exhibits this effect, which we attribute to a small number of modes with a substantial evanescent field extending outside the Yb-doped core. Still, in our simulations the rate of absorption is relatively high even when only 1% of the pump light remains, so the effect is not significant in practice.

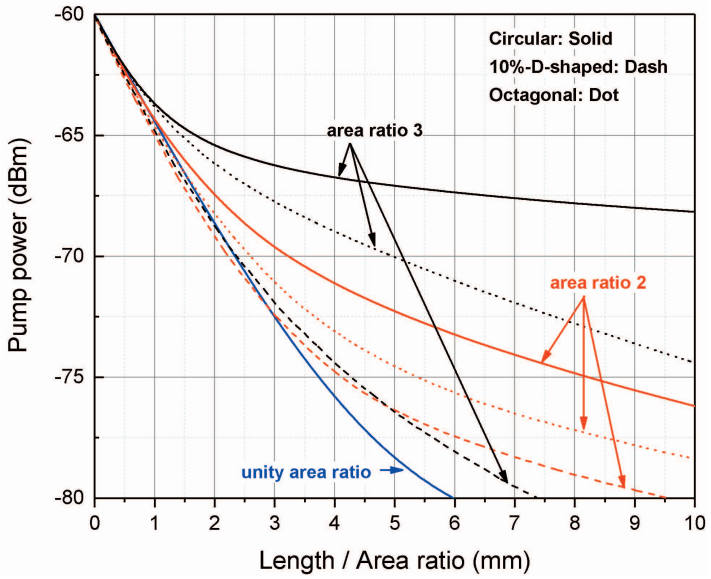

Fig. 2. Small signal absorption of pump vs. scaled fiber length for circular and non-circular inner cladding at different area ratios. Solid lines: circular inner cladding. Dashed lines: 10%-D-shaped inner cladding. Dotted lines: octagonal inner cladding.

Table 2 summarizes results presented throughout this paper, including these small-signal absorption characteristics. For the fibers with circular inner cladding, the absorption values for which the rate of absorption (i.e., the slope in Fig. 2) drops by half become 3.8 dB (58%) and 7.5 dB (82%) for cladding / core area ratios of 3 and 2, respectively. Furthermore, the absorptions for which the length required is twice as long as it would be with the uncompromised initial absorption become 4 dB (60%) and 7.7 dB (83%) for cladding / core area ratios of 3 and 2, respectively. We can describe this as if approximately 35% - 40% (area ratio 3) and 17% - 20% (area ratio 2) of the power have a poor overlap with the core, whereas the overlaps are reasonable for the remaining power. The fractions can be compared to the percentage of pump light launched outside the core area of 67% and 50%. Thus, the fraction of pump power with reasonable small-signal absorption significantly exceeds the core's area fraction.

Figure 2 and Table 2 also show the improvements possible with octagonal and 10%-D-shaped inner cladding. For D-shaping, a segment of 10% height relative to the diameter is removed from the otherwise circular inner cladding. D-shaping comes close to the ideal case even for area ratio of 3, for which the octagonal shape is less effective.

Optics EXPRESS

Table 2. Summary of Key Results.

	Area ratio	Transversally uniform distribution[1]	Circular BPM	Analytic / estimate[a]	Octagonal BPM	10%-D-shaped BPM
Length-scaling factor to reach 10 dB small-signal pump absorption relative to ideal case[1] (cf. Fig. 2 & 3)	1	1 (2 mm)	1	1[2]	Not considered[3]	Not considered[3]
	2	1 (4 mm)	1.6	10 dB not reached[2]	1.3	1.1
	3	1 (6 mm)	15.8	10 dB not reached[2]	2.5	1.2
Fraction of unabsorbed pump power where rate of absorption has dropped by half in small-signal regime (cf. Fig. 2 & 3)	1	0%	~0 %	0%	Not considered[3]	Not considered[3]
	2	0%	17.7%	33.3%[2]	7.2%	5.1%
	3	0%	41.7%	48.5%[2]	32.4%	5.7%
Residual pump power after 15 dB ideal pump absorption[1] in small-signal regime (cf. Fig. 2 & 3)	1	3.2%	~3.2 %	3.2%[2]	Not considered[3]	Not considered[3]
	2	3.2%	11%	21.2%[2]	7.8%	5.7%
	3	3.2%	23.6%	32.6%[2]	16.6%	6.4%
Residual pump power after infinite length (both small-signal and high-power case)	1	0	0	0[2]	0[3]	0[3]
	2	0	0	18.2%[4]	0	0
	3	0	0	30.8%[2]	0	0
Length and length-scaling factor relative to BPM calculation with unity area ratio for amplifier with 10 dB (27 W) operating pump absorption (cf. Fig. 4 & 6)	1	Same as analytic / estimate	52.3 mm 1	42.4 mm[5] 0.81	Not considered[3]	Not considered[3]
	2	Same as analytic / estimate	64.1 mm 1.22	44.5 mm[5] 0.85	55.19 mm 1.06	52.88 mm 1.01
	3	Same as analytic / estimate	165.5 mm 3.16	46.6 mm[5] 0.89	71.25 mm 1.36	60.45 mm 1.16
Signal output power and gain for amplifier with 10 dB (27 W) operating pump absorption (cf. Fig. 4 & 6)	1	Same as analytic / estimate	24.42 W 23.87 dB	24.4 W 23.87 dB	Not considered[3]	Not considered[3]
	2	Same as analytic / estimate	24.25 W 23.84 dB	Same[6]	23.67 W 23.74 dB	23.63 W 23.73 dB
	3	Same as analytic / estimate	24.13 W 23.82 dB	Same[6]	23.7 W 23.75 dB	23.79 W 23.76 dB
Effective length at 10 dB operating pump absorption	1	Not calculated	14.9 mm	9.06 mm[7]	Not considered[3]	Not considered[3]
	2	Not calculated	23.4 mm	10.78 mm[7]	15.85 mm	14.01 mm
	3	Not calculated	115.97 mm	12.5 mm[7]	26.46 mm	17.32 mm

[a] Either ray model with circular geometry or with transversally uniform power distribution (Eq. (2))

[1] Pump is transversally uniformly distributed in each fiber cross-section.

[2] From ray model, Eq. (15) & Fig. 3

[3] Our assumption of a circular core is at odds with a non-circular geometry with unity area ratio. If a non-circular core is considered then the results are expected to be close to those for a circular core.

[4] From ray model, Eq. (8) & Fig. 12

[5] Eq. (2) with 10 dB pump absorption and 23.87 dB signal gain.

[6] 90% power conversion efficiency with respect to absorbed pump power assumed, which can be compared to the quantum-defect-limited conversion efficiency of 976/1060 = 92.1%.

[7] Eq. (2) with 4.343 dB signal gain to 24.4 W of output power and 8.269 dB pump absorption to 3 W of pump leakage (15.42 W of added signal power and 17.14 W of absorbed pump power with 90% conversion efficiency).

Optics EXPRESS

As it comes to the required small-signal absorption, typical design targets are in the range 10-20 dB for typical double-clad fibers. Whereas the decrease in absorption rate along the fiber makes it difficult to reach 20 dB of absorption with a circular geometry, 10 dB is feasible. For the circular fibers in Fig.2, in case of an area ratio of 3, the length-scaling factor required to reach 10 dB absorption relative to the uncompromised initial slope becomes 15.8 which appears prohibitively large. However, for an area ratio of 2, this length-penalty factor drops to 1.6.

Ray tracing is sometimes used to evaluate the absorption in double-clad fibers [2, 17–19]. This is justified with the highly multimode nature of a large inner cladding. One attraction with a ray treatment is that it allows us to derive analytical expressions for the small-signal absorption in case of a circular inner cladding. See Appendix. However, since the inner claddings we consider are much smaller than in previous treatments [1, 15–17], and support much fewer modes, a ray model may not be appropriate. To investigate this, Fig. 3 and Table 2 present results of ray-based absorption calculations according to Eq. (8) and (15), together with the corresponding cases calculated with BPM from Fig. 2. We see that the ray treatment underestimates the absorption, as compared to the more accurate wave treatment of BPM. This is expected. There is a fraction of skew rays which would never interact with the core of an unperturbed circular fiber and would thus never be absorbed. However, a ray, without any transverse spread, is only an approximation of a physical beam of light, which will inevitably interact with the core as the light beam diffracts. (Equivalently, although a modal superposition can be phased so that it tightly confines the energy in one point, it dephases along the fiber so that the energy spreads out and interacts with the core.) Consequently, the ray treatment can be viewed as a lower bound on the actual absorption. According to Eq. (8), the fraction of rays that never interacts with the core becomes 30.8% (area ratio 3) and 18.2% (area ratio 2). This is in reasonable agreement with the fractions of power with poor absorption as evaluated with BPM. The ray approximation is expected to improve with larger structures. This is confirmed in Fig. 3 which includes BPM simulations of a fiber with area ratio 3, but scaled up in diameter by 2 and 4 times. This reduces the absorption and makes it closer to the ray calculations.

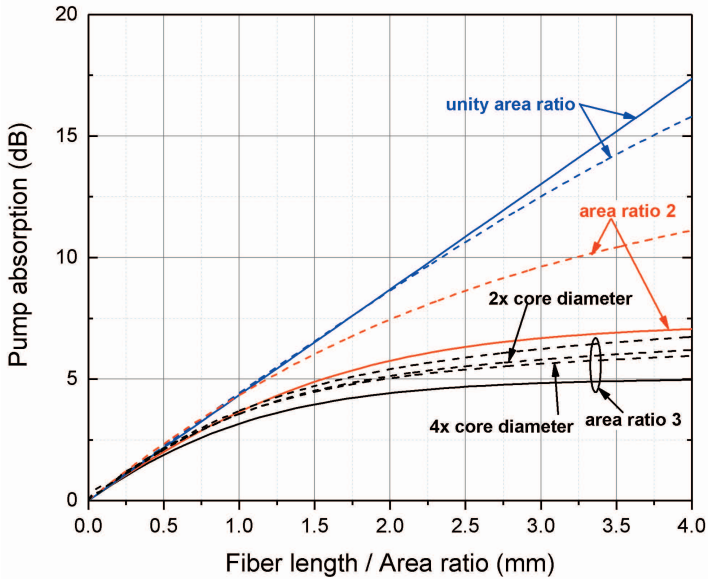

Fig. 3. Small signal pump absorption vs. scaled fiber length at different area ratios with circular inner claddings. Solid lines: analytical expressions in ray model. Dashed lines: beam propagation method. For area ratio of 3, fibers that are scaled up in core and cladding diameter by 2 and 4 times are included, in addition to the default case with parameters as given in Table 1.

Optics EXPRESS

3.2. Pump absorption in operating amplifier

The small-signal "cold" absorption is generally assumed to be closely linked to the required length and performance of a cladding-pumped fiber. However, the actual "hot" pump absorption, when the fiber is operating as an amplifier or a laser, is of more direct importance, and ultimately the conversion efficiency (or output power) and the signal's effective length for nonlinear interactions (e.g., stimulated Raman scattering) are often the primary parameters of interest. Given that a fraction (n_2) of the Yb-ions are excited in the operating fiber, the operating absorption becomes smaller than the "cold" absorption. Figure 4 shows how the pump and signal powers evolve for circular inner claddings. It is similar to Fig. 2, with parameters from Table 1, but in the high-power regime, with 30 W of launched pump power and 0.1 W of signal seed power. This will result in up to ~24 dB of gain in an efficient device, i.e., if most of the pump power is converted to signal power. There is no loss in our simulations, except for spontaneous emission. The pump power that needs to be absorbed to compensate for the spontaneous emission at 24 dB of gain becomes ~0.5 W. This power, which takes away from the conversion efficiency, is proportional to the effective area of the signal. (It also depends on the fiber length but because of the low "cold" absorption at the signal wavelength, this is negligible.) There are now three distinct regions, shown in Fig. 4. An initial region where the absorption is saturated by the strong pump is followed by one with a higher absorption where the signal power is sufficient to reduce the fraction of excited Yb-ions. In case of an area ratio of 3, there is also a final region with low absorption in which the pump power resides in modes with low overlap with the Yb-doped core. This impairs the conversion from pump to signal. By contrast, for an area ratio of 2, it is possible to convert nearly all the pump into signal even in a circularly symmetric fiber, according to our simulations.

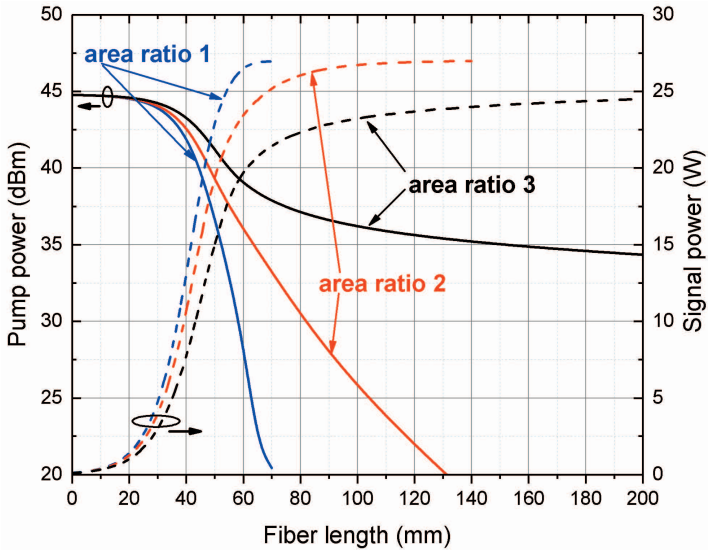

Fig. 4. Evolution of pump power (in dBm) and signal power (in W) in the high-power regime for circular inner claddings with different area ratios.

3.3. Fiber length

The required fiber length is also interesting , and closely related to the pump absorption. First, we reiterate that the lengths in our graphs are artificially short because of an artificially high Yb-concentration, but can be rescaled to longer lengths corresponding to lower Yb-concentrations

Optics EXPRESS

in Fig. 4 and elsewhere. In Fig. 4, the required length is only marginally longer with cladding-pumping than with core-pumping, except when pump modes with poor overlap with the core become dominant for area ratio of 3. Therefore, in contrast to the small-signal absorption plots, the length axis is no longer scaled by the area ratio. However, with all three area ratios, the fibers are much longer than suggested by the conventional target of 10-20 dB small-signal absorption. For example, for unity area ratio, an operating pump absorption of 10 dB is reached after 52.2 mm, at which point the small-signal absorption reaches 261 dB in the ideal case with perfect overlap.

To better understand the required fiber length in operating devices, we write the gain in decibels, G_{dB}, as [20]

$$G_{dB} = 4.343\Gamma N_0 L\left[(\sigma_e + \sigma_a)\, n_2 - \sigma_a\right], \tag{1}$$

Here, Γ is the overlap between the light-field and the doped region, N_0 is the Yb ion concentration, L is fiber length, n_2 is the fractional excitation of the Yb ions averaged along and across the fiber, and σ_e and σ_a are emission and absorption cross-sections. For the pump, the gain is negative and related to the operating pump absorption as $\alpha^{op}_{dB} = G_{dB}$, with a reduced overlap in case of cladding-pumping. It is straightforward to derive the following expression for how the length depends on the gain and operating absorption, where n_2 has been eliminated and where superscripts s and p designate quantities for the signal and pump:

$$L = \frac{G^s_{dB}\left(\sigma^p_a + \sigma^p_e\right) + r_{A\Gamma}\alpha^{op}_{dB}\left(\sigma^s_a + \sigma^s_e\right)}{4.343N_0\left(\sigma^p_a\sigma^s_e - \sigma^p_e\sigma^s_a\right)}, \tag{2}$$

Here, $r_{A\Gamma} = \Gamma^s/\Gamma^p$is the effective area ratio. (If we also assume that the signal overlap $\Gamma^s = 1$ and that the pump overlap Γ_p is equal to A_{core}/A_{clad} then $r_{A\Gamma}$ equals the geometric area ratio A_{clad}/A_{core}.) Note that often, $\sigma^p_a\sigma^s_e \gg \sigma^p_e\sigma^s_a$ in our case by a factor of 54 (and σ^s_e is larger than σ^s_a by a similar factor). Note also that for a conventional double-clad fiber with sufficiently large (effective) area ratio, the second term in the numerator dominates over the first term. This implies that the need to absorb the pump power dictates the fiber length. However, for smaller area ratios, the first term, and thus the need to achieve a certain signal gain, becomes more important. From Eq. (2), the length scales with the area ratio as follows:

$$\frac{L}{L_1} = \frac{r_{A\Gamma} - 1}{1 + \frac{G^s_{dB}/(\sigma^s_a+\sigma^s_e)}{\alpha^{op}_{dB}/(\sigma^p_a+\sigma^p_e)}} + 1, \tag{3}$$

where L_1 is the fiber length for $r_{A\Gamma} = 1$. Note that here, $r_{A\Gamma}$ is assumed to be independent of fiber length, whereas it could in general change due to changing pump power distribution. If $r_{A\Gamma} \gg 1 + \left[G^s_{dB}/\left(\sigma^s_a + \sigma^s_e\right)\right]/\left[\alpha^{op}_{dB}/\left(\sigma^p_a + \sigma^p_e\right)\right]$ (i.e., for large area ratio), or if $\left[G^s_{dB}/\left(\sigma^s_a + \sigma^s_e\right)\right]/\left[\alpha^{op}_{dB}/\left(\sigma^p_a + \sigma^p_e\right)\right] \ll 1$ (e.g., for low gain), then (L/L_1) is approximately proportional to $r_{A\Gamma}$. However, in other regimes the dependence on $r_{A\Gamma}$ is weaker. With our parameters, with cross-sections from Table 1, $\alpha^{op}_{dB} = 10\,\text{dB}$, and $G^s_{dB} = 24\,\text{dB}$, Eq. (3) becomes

$$\frac{L}{L_1} = \frac{r_{A\Gamma} - 1}{20.51} + 1, \tag{4}$$

Thus, for the area ratios we consider, the dependence on the area ratio is much weaker than proportional. Rather, increasing the area ratio from 1 to 2 only increases the fiber length by 4.8%. We emphasize that this assumes that the overlaps are constant along the fiber (e.g., if the transverse pump profile remains uniform). Note also that with our fiber parameters, the gain peaks at around 1030 nm rather than at 1060 nm (our signal wavelength). At 1030 nm, $(\sigma^s_a + \sigma^s_e)$ is considerably larger, so the dependence of L/L_1 on $r_{A\Gamma}$ is stronger. (The required fiber lengths are shorter, too.)

Optics EXPRESS

Deviations from a uniform pump beam profile and thus variations in the overlap with the Yb-ions along the fiber mean that even longer fibers are needed to reach a given operating absorption in a cladding-pumped fiber with a circular inner cladding. Still, the weak dependence on the area ratio in Eq. (2) - (4) remains influential. Thus, compared to the core-pumped case, the actual fiber length for 10 dB operating absorption at an area ratio of 2 is only 22% longer in the BPM calculations of Fig. 4. By contrast, in case of an area ratio of 3, the large fraction of pump power in modes with poor overlap with the core means that we reach 10 dB of absorption only for an actual length of 165.5 mm, which is 3.16 times the length with core-pumping. However, a shaped cladding makes the transverse pump distribution more uniform and improves the applicability of Eq. (1) - (4) also with area ratios of three and larger.

3.4. Effective length

It is clear from above that fibers with small area ratio need to be significantly longer than suggested by simple scaling by the area ratio from typical values in a double-clad fiber (e.g., 100). On the other hand, the signal's effective length, L_{eff}, which is related to nonlinear degradation, is often more important than the actual fiber length. We have,

$$L_{eff} = \frac{\int_0^L P(z)\,dz}{P(L)}, \tag{5}$$

where $P(z)$ is the signal power along the fiber. Figure 5 plots the effective length vs. the actual length as well as the output power $P(L)$, for the same conditions as in Fig. 4. The effective lengths are much shorter than the actual lengths, but are still generally many times larger than the "cold" pump absorption length. According to Eq. (2), under the simplification of transversally uniformly distributed pump and signal, the actual length becomes $L = 1.69G^s_{dB} + 0.208r_{A\Gamma}\alpha^{op}_{dB}$ [mm] with our parameters. Thus, with our parameters, a gain of ~24 dB influences the length more than an operating pump absorption of, say, 10 dB does, for area ratios between 1 and 3, and it is again clear that a requirement for high gain strongly influences the fiber length. However, it does not necessarily strongly influence the effective length. When the signal power becomes high and makes the integrand in Eq. (5) significant, it will at the same time reduce the Yb-excitation and thus improve the pump absorption. Remaining pump power in modes with adequate overlap with the Yb-ions can then be absorbed and converted to signal in a relatively short distance, which reduces the effective length. The effective length can be approximated as the length over which the signal gain reaches 4.343 dB as measured from the signal output end. In an efficient device with 90% conversion of absorbed pump into signal and 10% (3 W) pump leakage, the signal output power becomes 24.4 W. The final 4.343 dB of gain corresponds to 15.4 W of generated signal power from 17.1 W of absorbed pump (with 90% efficiency). It follows that the pump absorption in this last section becomes 8.27 dB. Thus, more than 80% of the total pump absorption in decibels occurs in this length, which is approximately equal to the effective length. From Eq. (2), it becomes 9.1 - 12.5 mm for area ratios 1- 3. See Table 2.

For $r_{A\Gamma} = 2$, the effective-length estimate becomes 10.8 mm. This deviates by a factor-of-two from the 90%×90%=81% conversion point (24.4 W of output power) in Fig. 5. The deviation is smaller for $r_{A\Gamma} = 1$. This suggests that pump power in modes with poor overlap with the core causes the deviation, which should therefore become smaller with shaped claddings. Figure 6 compares the power evolution and Figure 7 compares the effective length between the same circular inner claddings as used in Fig. 4 with shaped inner claddings, at area ratio of 2 and 3. The agreement with our simple estimate is better with shaped claddings. The Figs also confirm that an area ratio of two works well with a circular geometry. The effective length becomes larger at an area ratio of 3, especially for high conversion efficiency with circular inner cladding. Other curves are closer together, with relative separation smaller than the separation in area ratio. We conclude that as for the actual length of an operating fiber, the effective length does not depend

Optics EXPRESS

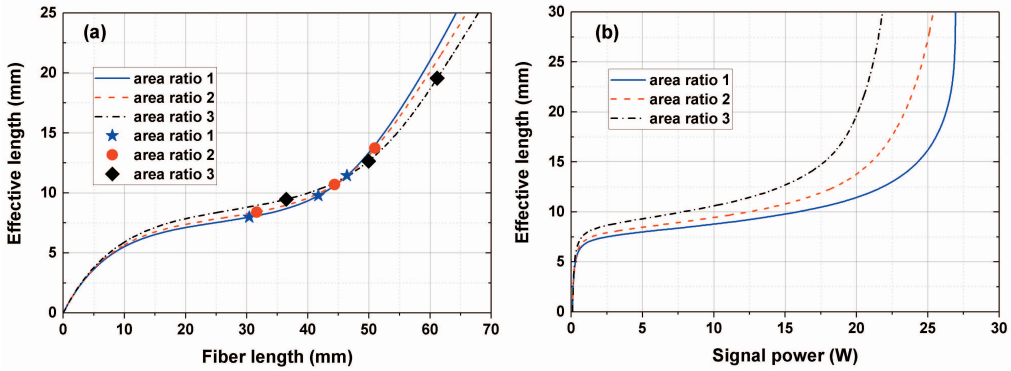

Fig. 5. Effective length of signal for circular inner claddings with different area ratios as a function of (a) actual length and (b) signal output power. Signal output powers of 5, 15, and 20 W are also marked in (a), where lower output powers have shorter effective length.

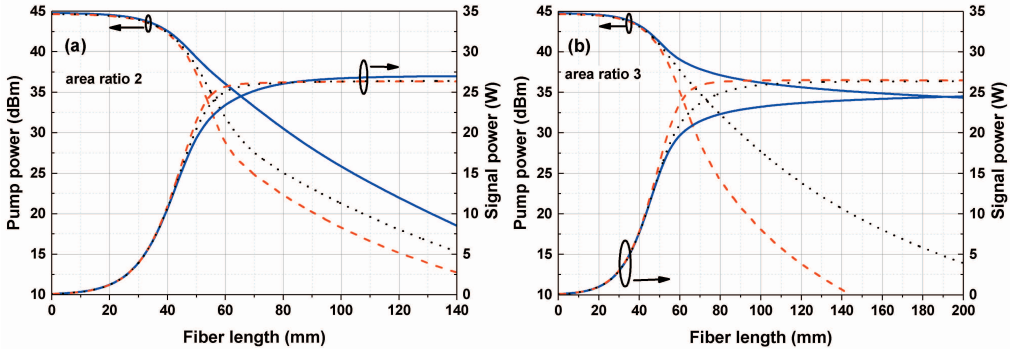

Fig. 6. Pump and signal power along the fiber for circular (solid, blue), 10%-D-shaped (dashed, red) and octagonal (dotted, black) inner cladding at (a) area ratio 2 and (b) area ratio 3.

strongly on the fiber geometry for the parameters we considered, provided that the fraction of pump power with poor absorption is small.

3.5. Scaling considerations

BPM is computation-intensive, and we therefore restrict the simulations to short fibers with relatively small core and inner cladding. We next discuss to what extent the simulations are valid for other fiber parameters. Although we only consider a small set of scaling cases, these can be combined to other cases not explicitly treated.

In some cases, it is possible to exactly scale results. The results depend on the dephasing and saturated amplification and absorption of modes. If the core and inner-cladding dimensions are both scaled by a factor of x (so the area ratio stays the same), and their respective NA are scaled by x^1 so that their V-values remain constant, then the modal dephasing along the fiber remains constant if the length is scaled by x^2. If also the Yb-concentration is scaled to yield the same absorption in the scaled length (so by x^2), and the pump and signal powers are scaled by x^2 to yield the same intensities and thus the same Yb-excitation, then the pump- and signal-field evolutions remain identical, except for the scaling. Simulations confirmed this. Also, to repeat, if the spontaneous emission rates and thus the intrinsic signal saturation power are comparatively

Optics EXPRESS

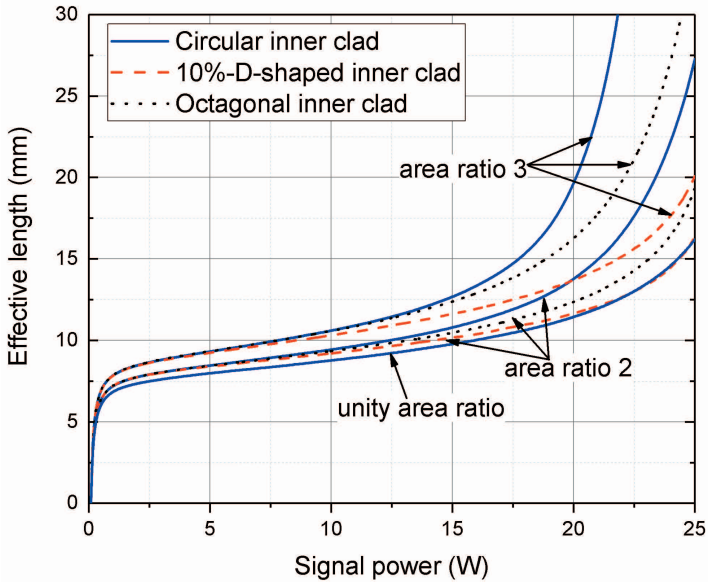

Fig. 7. Effective length *vs.* signal output power for circular (solid, blue), 10%-D-shaped (dashed, red) and octagonal (dotted, black) inner cladding at area ratio 2 and 3.

small, then the ratio of the signal and pump power matters more than their absolute values. Note however that we neglect mode-coupling. This increases in larger waveguides, and then the results are no longer perfectly scalable.

For the parameters we considered, we also found that the length had no effect if the Yb-concentration was changed to keep the concentration-length product constant. This would not be the case, if the interaction of mode beating and local gain saturation is significant and not averaged out because the fiber is too short, but we saw no such effect.

To investigate scaling that keeps the area ratio constant, we next compare the results for the circularly symmetric fiber with area ratio of two, and already plotted in Fig. 4, with those for another fiber with the same core V-value, area ratio, and inner-cladding NA but with core diameter and thus inner-cladding diameter which are twice as large. We also scaled the pump and signal input power to keep the power density the same. The simulations show that even when the area ratio is constant, a larger inner cladding reduces the pump absorption and the signal power. See Fig. 8. This is understandable. The larger inner cladding has a larger V-value and thus supports more modes. From Fig. 8, we conclude that some of these modes have small overlap with the Yb-doped core and therefore are only slowly absorbed, although the effect is relatively small with our parameters. A larger inner-cladding NA increases the number of pump modes, too, and is also expected to increase the problem of pump modes with poor overlap in a circular geometry. However, an inner-cladding NA of 0.3 is already high for all-glass fibers. A higher inner-cladding NA may not be realistic in high-silica fibers suitable for high-power operation.

3.6. Signal mode purity

Unlike conventional DCFs with a large area ratio, the overlap between cladding-modes of the signal and the Yb-doped core cannot be neglected in small-area-ratio fibers. Table 3 lists the overlap between the Yb-doped core and the signal-modes LP_{01}, LP_{11}, and LP_{02} for area ratios of 1, 2, 3, and 100. The latter is a more conventional geometry for which only LP_{01} has significant overlap with the core. For area ratio 2 and 3, the overlaps and thus the gains of the cladding-guided higher-order modes (HOMs) LP_{11} and LP_{02} are significant even though the V-value of the core

Optics EXPRESS

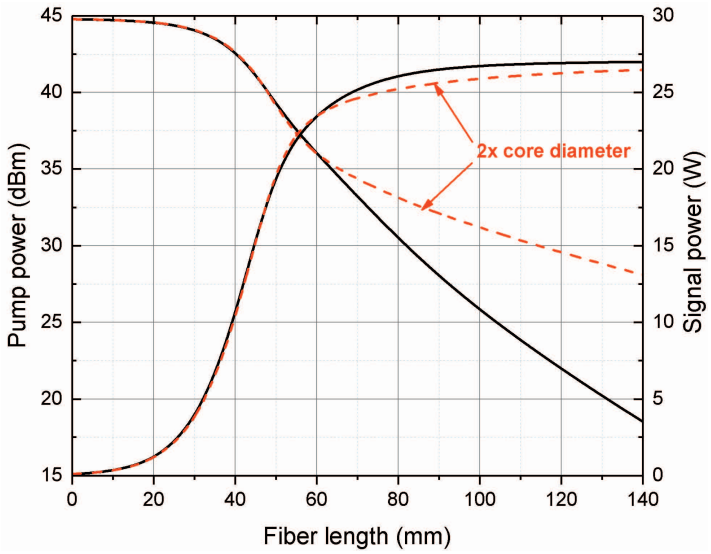

Fig. 8. Power evolution for fibers with area ratio of 2 selected from Fig. 4 (solid, black); with core and cladding diameters which are twice as large (dashed, red). The pump and signal powers for the larger-diameter case are scaled to yield the same power density as for the smaller default diameters.

is below the cutoff for SM operation. This can degrade the mode purity. To investigate this, we excited both LP_{01} (95% of launched power) and LP_{11} (5% of launched power) with signal light at the input of the fiber for the simulations in Fig. 4. For the 140 mm long circular DCF at area ratio of two, the gain of the fundamental mode LP_{01} becomes 24.3 dB and the gain of LP_{11} becomes 21.7 dB. At area ratio of three with length of 210 mm, the gain becomes 24.1 dB and 18.0 dB, respectively. We also used a mixture of all guided modes as signal input for the simulation where 90% of the signal power is in LP_{01}, and 10% of the signal power is in all HOMs with equal power and random phase. The gain of the fundamental mode LP01 becomes 24.6 dB and the average gain of the HOMs becomes 17.7 dB at area ratio of two. At area ratio of three, the gain values become 24.3 dB and 12.8 dB, respectively. Thus, we find the mode purity improves after amplification in all cases, as shown in Fig. 9. However, the gain difference between LP_{01} and higher-order modes is much smaller than in a conventional single-mode double-clad fiber, which makes the signal launch more critical. It is also interesting to note that the fraction of power in LP_{01} reaches equilibrium values which are different for the different cases, but less than unity. We attribute this to LP_{01}'s weak compression of the gain in the edges of the core [10]. This leads to higher gain of the HOMs, until they reach an equilibrium where they saturate the gain to the level of LP_{01}. The power in the HOMs is higher for smaller area ratios. Still the signal output was close to diffraction limited (M^2 = 1.12) even at an area ratio of 1.5. Note that our simulations are for straight fibers and the details are expected to change for bent fibers. Furthermore, simulations showed that the D-shaped fiber, which has the lowest symmetry of the geometries we consider, had a slightly worse LP_{01} equilibrium power-fraction. Note also that in Table 3, the difference in modal effective index between LP_{01} and the HOMs is smaller in the double-clad fibers with single-mode core than in the fiber with the multimode core. We mention also that significant gain for HOMs can promote transverse mode instability [21, 22].

Optics EXPRESS

Table 3. Overlap, Effective Index, and Output Power in Different Modes for Different Area Ratios for Circularly Symmetric Fibers.

Area ratio	LP_{01} overlap / effective index	LP_{01} final power fraction (from Fig. 4)	LP_{11} overlap / effective index difference to LP_{01}	LP_{02} overlap / effective index difference to LP_{01}
1	0.998 / 1.4399877		0.995 / 1.35×10^{-3}	0.989 / 3.66×10^{-3}
2	0.919 / 1.4403246	0.978[1] / 0.959[2]	0.809 / 0.81×10^{-3}	0.67 / 2.17×10^{-3}
3	0.861 / 1.4403875	0.992[1] / 0.983[2]	0.658 / 0.67×10^{-3}	0.444 / 1.64×10^{-3}
100	0.794 / 1.44042		0.047 / 0.439×10^{-3}	0.003 / 0.4394×10^{-3}

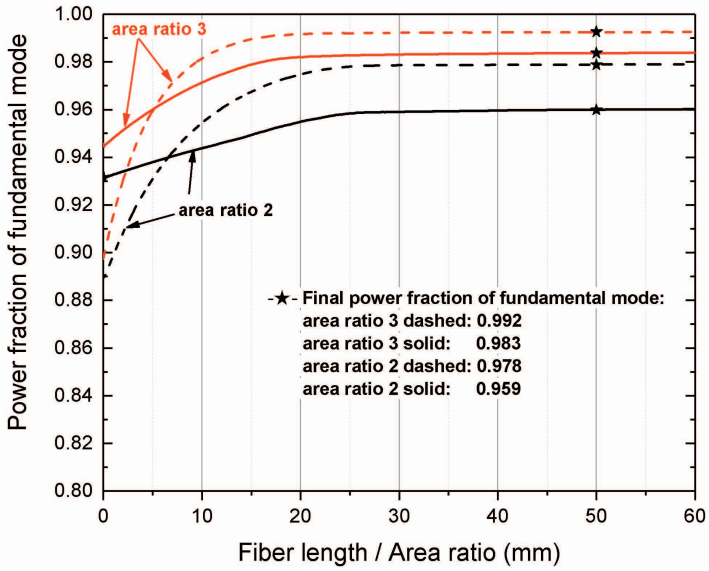

Fig. 9. Power fraction of fundamental mode for different signal seed profiles, but with same total seed power. Solid line: mixture of modes LP_{01} and LP_{11} where the phase difference of LP_{01} and LP_{11} is zero and where 5% of the power is in LP_{11}; Dashed line: mixture of modes LP_{01} and all other guided modes where the phases of LP_{01} and high-order-mode are random and where a total of 10% of the power is in all HOMs with equal power.

3.7. *Other operating regimes*

Pumping at shorter wavelengths than the peak at 976 nm (e.g., 915 - 940 nm) makes the dependence of the length on $r_{A\Gamma}$ stronger. In these regimes, the excitation level n_2 is smaller, which also reduces the difference between the small-signal and the high-power pump absorption. In addition, the difference between pumping on and off the absorption peak may be smaller when the length is primarily determined by the need to reach adequate gain. However, in case of tandem-pumping at wavelengths longer than the absorption peak (1018 nm is often considered), the factor $(\sigma_a^p \sigma_e^s - \sigma_e^p \sigma_a^s)$ in the denominator of Eq. (2) can be small. Longer fibers are then needed, although the absorption can still be adequate with realistic Yb-concentrations. For example, $r_{A\Gamma} = 2$ requires a total of 1485 dB of small-signal core absorption at 976 nm for 10

Optics EXPRESS

dB operating absorption at 1018 nm and 24 dB gain at 1060 nm, according to Eq. (2). This is comparable to the core absorption of a conventional cladding-pumped fiber. A full investigation of the impact of different signal and pump wavelengths at small area ratios is beyond the scope of this paper. We also mention that cladding-pumped fiber Raman amplifiers and lasers benefit from area ratios of at most ~8 [23]. Our simulations here suggest that the efficiency would improve with even smaller area ratio, given that fibers are typically circularly symmetric for ease of manufacture. Experiments confirm that residual pump power has low overlap with the core in a circularly symmetric double-clad Raman fiber with area ratio ~5.8 [23].

4. Conclusions

We have used BPM and rate equations to simulate the pump absorption, signal amplification, mode purity, and effective length of the signal in co-directionally cladding-pumped Yb-doped fiber amplifiers with a single-mode core in a small inner cladding (area ratio between cladding and core of 1 - 3), as well as in comparable core-pumped multimode fibers. This is relevant for the design of cladding-pumped fibers and lasers and amplifiers with small area ratios and high-brightness pumping. We have primarily considered a pump wavelength of 976 nm and a signal wavelength of 1060 nm. Table 1 lists our default fiber parameters and Table 2 summarizes key results.

We assumed that mode-coupling is negligible, which is reasonable with the small inner-cladding diameters we considered (typically 20-30 μm). The absence of mode-coupling reduces the absorption when there are pump modes with low overlap with the Yb-doped core, and this is a concern in fibers with a circular inner cladding. Nevertheless, we found that the pump absorption was acceptable even with a circular inner cladding for area ratios up to ~2.5, in fibers with ~23.7 μm diameter, 0.3-NA inner cladding. As it comes to the small-signal pump absorption, this was then deemed sufficiently close to exponential up to 10 dB or more, and the absorption rate was reasonably close to the inverse of the area ratio. The pump absorption degraded with larger area ratios, but recovered when the circular symmetry was broken with D-shaped and octagonal inner claddings. Such geometries are often used for conventional fibers with large area ratio, but are difficult to combine with some fabrication approaches for small-area-ratio fibers. We also derived ray-model-based analytic expressions for the small-signal absorption in circular structures. This underestimates the absorption, but still shows that more than 75% of the power is in rays that are absorbed for area ratios smaller than 2.5, *vs.* only 13% for a typical area ratio of 100. The ray calculations agree better with the more accurate BPM simulations for larger inner claddings that support more modes.

The inner-cladding parameters that worked well for the small-signal pump absorption agree with those that worked well for the more relevant "hot" (operating) pump absorption in the high-power regime. However, the excitation of Yb-ions is significant in a fiber with small area ratio. We showed analytically that consequently, a need for high gain (e.g., ~24 dB in our case) is more important for the required fiber length than the need for adequate pump absorption. This reduces the benefits of a small inner cladding. On the other hand, we showed that the dependence on the effective length for nonlinear interaction is relatively stronger, although still much weaker than the small-signal absorption's ideally inverse dependence on the area ratio. Furthermore, it is still generally possible to achieve short as well as typical targeted fiber lengths by adjusting the Yb-concentration and thus expand the engineering control of the length.

We discussed the impact of scaling fiber parameters within a fixed area ratio. Increasing the inner cladding to 84.9 μm diameter at an NA of 0.3 and an area ratio of 2 did show some degradation in the absorption, but the effect was modest. We attribute this degradation to the appearance of modes with increasingly low overlap with the core, as the number of guided modes increases. The Yb-concentration was not important, if the concentration-length product is kept constant. Thus, it is possible to scale the fiber lengths we report to other values, in inverse

Optics EXPRESS

proportion to the Yb-concentration. Nevertheless, many fiber parameters will influence the results, and their importance depends on factors such as cladding geometry, operating regime (e.g., gain level) and spectroscopy (including the case of other active dopants). The reduced importance of the pump absorption for the fiber length may also make it less beneficial to pump on the absorption peak. We have not simulated tandem-pumping on the long-wavelength side of the absorption peak (e.g., at 1018 nm). However, we expect that key conclusions still apply, and that adequate pump absorption is possible also in those cases, although the required fiber length may be comparable to that for a conventional double-clad fiber.

The presence of cladding-modes with high overlap with the core affects the mode purity in circular fibers with small inner cladding. Although the signal gain remains the highest for the fundamental mode so that some signal-mode purity enhancement relative to the launch signal is possible, the gain for cladding-guided higher-order modes can be nearly as high. Furthermore, mode-selective gain saturation leads to an equilibrium distribution with a few percent of the signal power in higher-order modes. Still, even though a circular inner cladding suffers from reduced absorption already at an area ratio of three and a smaller inner cladding may increase the signal power in higher-order modes, there is a range of area ratios that allow for good pump absorption and good beam quality even in circular inner claddings.

Appendix: Ray approximation for pump absorption

Figure 10 shows the double-clad fiber structure we consider, with concentric inner cladding and doped region (coinciding with the core) with radius a relative to the inner cladding and with uniform Yb-concentration. This is essentially the same as for the BPM calculations. The area ratio becomes a^{-2}. However, in the ray modeling, we neglect refraction in the core and effectively treat a medium with constant refractive index within the inner cladding. We also assume that the pump-rays are reflected at a "hard" outer boundary of the inner cladding. After each reflection, a ray will travel an equivalent path through the inner cladding until it reaches the cladding boundary again. In doing so, it may pass through the core, whereby a fraction of the power in the ray is absorbed. Other rays will not pass through the core. The circular geometry means that the path of a reflected ray will be equivalent to the path of the incident ray, so it is enough to treat a single pass of a ray through the cladding. The circular geometry also means that it is sufficient to characterize a ray by its minimum distance x to the center of the fiber, the inner caustic [24],since rays traveling at different angles in the cross-sectional (transverse) plane but have the same minimum distance have the same absorption. This is true even if the rays have different angles to the cross-sectional plane (and thus to the fiber axis): As a ray propagates down the fiber, the absorption of light in that ray is proportional to the fraction b of the path which is inside the Yb-doped region. This fraction, i.e., the overlap of a ray with the core, is independent of the angle of the ray to the cross-sectional plane (if refraction is neglected). Rays parallel to the fiber axis fall outside this description, but the fraction of the power in such rays is zero and they can therefore be disregarded. In addition, we disregard the longer path of rays propagating at larger angles to the fiber axis. This increases the absorption per unit length, but through a lower group velocity rather than a larger overlap, and only by ~2.2 % for a ray propagating at an angle of 0.20 rad to the fiber axis, corresponding to an NA of 0.3.

From Fig. 10, the overlap is given by $b = l/L$, where l is the length of the ray through the doped region as projected onto the transverse plane and L is the total (similarly projected) length of the ray through the inner cladding (including core), i.e., the chord. We have, from Pythagoras,

$$L = 2\left(1 - x^2\right)^{1/2}. \tag{6}$$

Optics EXPRESS

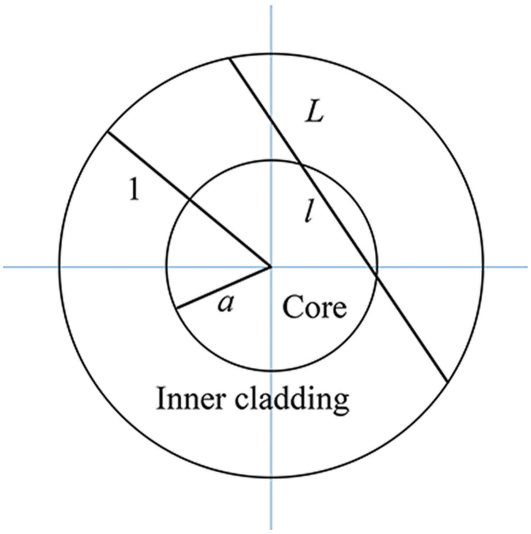

Fig. 10. Fiber cross-section and symbol definitions.

Using a similar expression for l, we can write b as follows:

$$\begin{aligned} b &= \left(a^2 - x^2\right)^{1/2} / \left(1 - x^2\right)^{1/2} && x < a \\ b &= 0 && x > a. \end{aligned} \tag{7}$$

We next consider the distribution of pump power between rays with different values of x. We assume that the fiber is excited uniformly, with uniform power density across the launch facet and with a uniform power distribution across the transverse angles. Note that this means that we exclude rays with complementary angle to the optical axis (i.e., angle to the transverse plane) which is below the critical angle for total internal reflection at the waveguide boundary. Although the angle to the transverse plane is equal to the angle of incidence for $x = 0$, it is smaller than the angle of incidence for $x > 0$. Specifically, the critical angle for total internal reflection internally in the core, θ_c, fulfills $\sin\theta_c = n_{core}/n_{clad}$. From this one may think that for $x > n_{core}/n_{clad}$ ($\approx$0.98 for an NA of 0.3), even rays perpendicular to the optical axis are supported in the ray model. However, because of the curvature of the core-cladding boundary, this is not the case, and only rays with complementary angle to the transverse plane larger than the critical angle, and thus within the NA of the core, are supported without loss [25]. A skew ray which does not fulfill this but still has angle of incidence larger than the critical angle is known as a tunneling ray, and is leaky [25]

Under these assumptions, the total power in rays with minimum center-distance x is proportional to L. The reason is that the intensity is everywhere uniform, so the power in any cross-sectional area is proportional to the size of the area. This includes a ray, which can be described as an infinitesimally thin rectangle. The fraction p_0 of the launched light that has zero overlap with the core can then be evaluated as the unshaded fraction of the total area in Fig. 11(a). We get

$$p_0 = 1 - (2/\pi)\left[a\left(1 - a^2\right)^{1/2} + \arcsin a\right], \tag{8}$$

This fraction of power will not be absorbed, according to this ray model, and is plotted in Fig. 11(b).

Optics EXPRESS

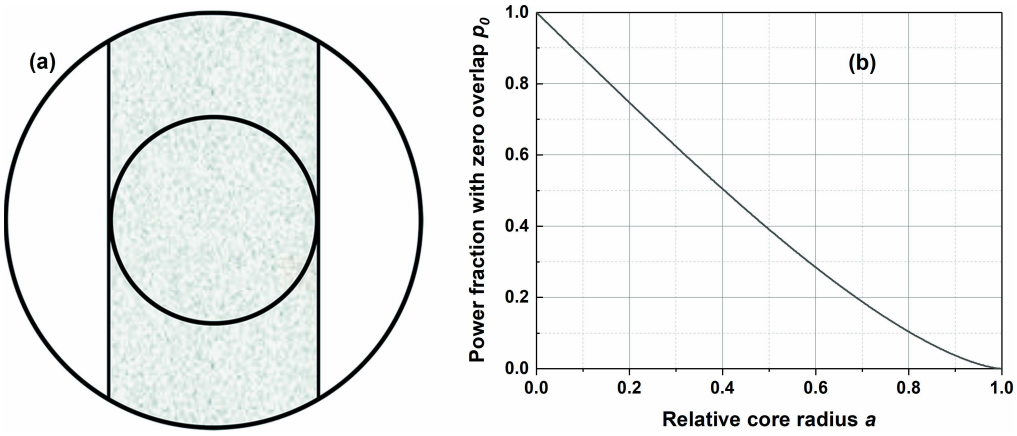

Fig. 11. (a) Fiber cross-section where shaded area represents fraction of power with non-zero overlap with core. (b) Fraction of power with zero overlap with core p_0 *vs.* relative core radius a.

To evaluate the distribution of rays with non-zero overlap, we first invert Eq. (7) to write x as a function of b.

$$x = \left(a^2 - b^2\right)^{1/2} / \left(1 - b^2\right)^{1/2} \qquad b < a. \tag{9}$$

For $0 < b < a$, the unscaled power distribution as a function of overlap b, $f_1(b)$, can then be found as follows:

$$\begin{aligned} f_1(b) &= h(b)\, dx/db \\ &= \left[\left(1 - a^2\right) / \left(1 - b^2\right)\right]^{1/2} b \left(1 - a^2\right) \left(1 - b^2\right)^{-3/2} \left(a^2 - b^2\right)^{-1/2} \\ &= b \left(1 - a^2\right)^{3/2} \left(1 - b^2\right)^{-2} \left(a^2 - b^2\right)^{-1/2} \qquad b < a, \end{aligned} \tag{10}$$

Here, $h(b) = \left[\left(1 - a^2\right) / \left(1 - b^2\right)\right]^{1/2}$ is the length of a ray (i.e., the relative power in a ray) with an overlap of b.

For normalization, we note that the fraction of the power with $b > 0$ is given by 1-p_0. Thus,

$$f(b) = (1 - p_0)\, f_1(b) / I_1, \tag{11}$$

where I_1 is the integral of $f_1(b)$ for $0 < b < 1$ (with $f_1 = 0$ for $b > a$). Although the distribution function diverges for $b = a$ (and for $b = 0$, with $f(0) = p_0\, \delta(0)$), the integral still converges. We have

$$I_1 = \left[a \left(1 - a^2\right)^{1/2} + \arcsin a\right] / 2. \tag{12}$$

Together, Eq. (8), (11), and (12) yield an analytic expression for the distribution of power *vs.* overlap $f(b)$. Thus,

$$\begin{aligned} f(b) = &\left[1 - (2/\pi) \left(a \left(1 - a^2\right)^{1/2} + \arcsin a\right)\right] \delta(b) + \\ &(4b/\pi) \left(1 - a^2\right)^{3/2} \left(1 - b^2\right)^{-2} \left(a^2 - b^2\right)^{-1/2} \qquad b < a, \end{aligned} \tag{13}$$

$$F(b) = \int_0^1 f(b')db'. \tag{14}$$

Optics EXPRESS

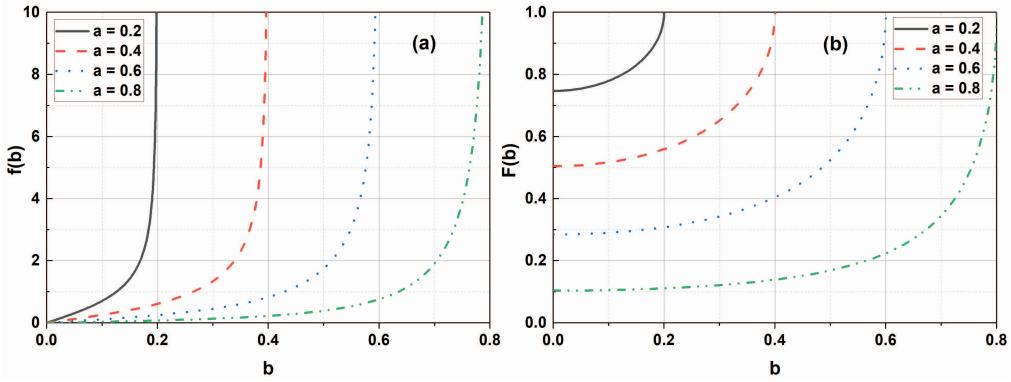

Fig. 12. Distribution of power $f(b)$ (a, left) and cumulative distribution of power $F(b)$ (b, right) *vs.* overlap b for relative core radius a = 0.2, 0.4, 0.6, and 0.8.

Figure 12 plots the distribution of power $f(b)$ and the cumulative distribution of power $F(b)$.

This derivation is not intuitive, and we therefore performed Monte-Carlo calculations with randomly generated rays, i.e. with random positions and directions in the transverse plane. These showed no discernible difference between Eq. (8), (13) and (14).

It is now straightforward to calculate the non-exponential evolution of the power. If we scale the parameters for unity core absorption and unity initial power then the power evolution becomes

$$p(z) = \int_0^1 f(b) e^{-bz} db. \tag{15}$$

This can also be scaled for unity initial absorption rate (independent of area ratio), and the result is plotted in Fig. 13.

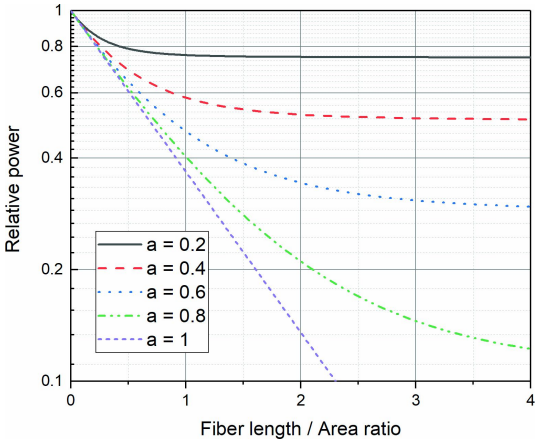

Fig. 13. Power evolution for a = 0.2, 0.4, 0.6, 0.8, and 1, in log scale.

Funding

Air Force Office of Scientific Research (AFOSR, FA9550-15-1-0041); The University research program of Northrop Grumman; Engineering, Physical Sciences Research Council (EPSRC,

Optics EXPRESS

EP/P001254/1); National Council for Science and Technology of Mexico (CONACyT, 578927/409382).

Acknowledgements

We thank Dr. Christophe A. Codemard, SPI laser, for helpful discussions.

References

1. S. Bedö, W. Lüthy, and H. Weber, "The effective absorption coefficient in double-clad fibres," Opt. Commun. **99**, 331–335 (1993).
2. A. Liu and K. Ueda, "The absorption characteristics of circular, offset, and rectangular double-clad fibers," Opt. Commun. **132**, 511–518 (1996).
3. A. Liu and K. Ueda, "Propagation losses of pump light in rectangular double-clad fibers," Opt. Eng. **35**, 3130–3134 (1996).
4. M. H. Muendel, "Optimal inner cladding shapes for double-clad fiber lasers," in *Conference on Lasers and Electro-Optics,* vol. 9 of *OSA Technical Digest* (Optical Society of America, Anaheim, California, 1996), p. CTuU2.
5. A. A. M. Saleh, R. M. Jopson, J. D. Evankow, and J. Aspell, "Modeling of gain in erbium-doped fiber amplifiers," IEEE Photonics Technol. Lett. **2**, 714–717 (1990).
6. T. Yao, J. Ji, and J. Nilsson, "Ultra-low quantum-defect heating in ytterbium-doped aluminosilicate fibers," J. Light. Technol. **32**, 429–434 (2014).
7. J. Nilsson, J. D. Minelly, R. Paschotta, A. C. Tropper, and D. C. Hanna, "Ring-doped cladding-pumped single-mode three-level fiber laser," Opt. Lett. **23**, 355–357 (1998).
8. F. Roeser, C. Jauregui, J. Limpert, and A. Tünnermann, "94 W 980 nm high brightness Yb-doped fiber laser," Opt. Express **16**, 17310–17318 (2008).
9. J. Boullet, Y. Zaouter, R. Desmarchelier, M. Cazaux, F. Salin, J. Saby, R. Bello-Doua, and E. Cormier, "High power ytterbium-doped rod-type three-level photonic crystal fiber laser," Opt. Express **16**, 17891–17902 (2008).
10. C. A. Codemard, J. K. Sahu, and J. Nilsson, "Tandem cladding-pumping for control of excess gain in ytterbium-doped fiber amplifiers," IEEE J. Quantum Electron. **46**, 1860–1869 (2010).
11. J. D. Minelly, R. I. Laming, J. E. Townsend, W. L. Barnes, E. R. Taylor, K. P. Jedrzejewski, and D. N. Payne, "High-gain fiber power amplifier tandem-pumped by a 3-W multistripe diode," in *Digest of Conference on Optical Fiber Communication,* (Optical Society of America, 1992), p. TuG2.
12. C. Unger and W. Stocklein, "Investigation of the microbending sensitivity of fibers," J. Light. Technol. **12**, 591–596 (1994).
13. D. J. DiGiovanni and R. S. Windeler, "Article comprising an air-clad optical fiber," U.S. patent 5,907,652, (May 25, 1999).
14. J. K. Sahu, C. C. Renaud, K. Furusawa, R. Selvas, J. A. Alvarez-Chavez, D. J. Richardson, and J. Nilsson, "Jacketed air-clad cladding pumped ytterbium-doped fibre laser with wide tuning range," Electron. Lett. **37**, 1116–1117 (2001).
15. J. Nilsson and D. N. Payne, "High-power fiber lasers," Science **332**, 921–922 (2011).
16. P. E. Lagasse and R. Baets, "Application of propagating beam methods to electromagnetic and acoustic wave propagation problems: A review," Radio Sci. **22**, 1225–1233 (1987).
17. H. Zellmer, A. Tünnermann, H. Welling, and V. Reichel, "Double-clad fiber laser with 30 W output power," in *Optical Amplifiers and Their Applications,* (Optical Society of America, 1997), p. FAW18.
18. A. Ankiewicz and C. Pask, "Geometric optics approach to light acceptance and propagation in graded index fibres," Opt. Quantum Electron. **9**, 87–109 (1977).
19. A. Ankiewicz and C. Pask, "Tunnelling rays in graded-index fibres," Opt. Quantum Electron. **10**, 83–93 (1978).
20. Y. Feng, B. M. Zhang, J. Zhao, S. Zhu, J. H. V. Price, and J. Nilsson, "Absorption measurement errors in single-mode fibers resulting from re-emission of radiation," IEEE J. Quantum Electron. **53**, 1–11 (2017).
21. T. Eidam, C. Wirth, C. Jauregui, F. Stutzki, F. Jansen, H.-J. Otto, O. Schmidt, T. Schreiber, J. Limpert, and A. Tünnermann, "Experimental observations of the threshold-like onset of mode instabilities in high power fiber amplifiers," Opt. Express **19**, 13218–13224 (2011).
22. M. N. Zervas and C. A. Codemard, "High power fiber lasers: A review," IEEE J. Sel. Top. Quantum Electron. **20**, 219–241 (2014).
23. J. Ji, C. A. Codemard, and J. Nilsson, "Analysis of spectral bendloss filtering in a cladding-pumped W-type fiber Raman amplifier," J. Light. Technol. **28**, 2179–2186 (2010).
24. A. W. Snyder and J. D. Love, *Optical waveguide theory* (Chapman and Hall, 1983), chap. 2.2.
25. A. W. Snyder and J. D. Love, *Optical waveguide theory* (Chapman and Hall, 1983), chap. 2.7.